



Wood powder characteristics of green milling with the multi-blade shaft mill

Atanu Kumar Das^{*}, David A. Agar, Mikael Thyrel, Magnus Rudolfsson

Swedish University of Agricultural Sciences, Department of Forest Biomaterials and Technology, SE-901 83 Umeå, Sweden

HIGHLIGHTS

- Investigation of wood powders made from green wood via a new one-step technology.
- Produced powders had much finer particle sizes than from attritional milling techniques.
- Particle properties include large surface area, more spherical shape and high porosity.
- Finer particles with spherical shapes had an influence on bulk density.
- The technology enables tailor-made particle size distributions for downstream processes.

GRAPHICAL ABSTRACT



ARTICLE INFO

Keywords:

Powder technology
Pinus sylvestris L.
 Aspect ratio
 Sphericity
 Image analysis
 Particle morphology

ABSTRACT

The quality of wood powders depends on the size reduction technology used to produce them. The pre-drying, chipping, and conventional (impact and attritional) size reduction steps, commonly employed in industry, act to degrade wood and diminish its full potential as a renewable feedstock. In this study, the effect of using a new green (i.e. freshly harvested) milling technology, the multi-blade shaft mill (MBSM), on wood powder properties was investigated. Particle size distribution (PSD) and shape properties were measured by two-dimensional image analysis and surface area analysis was performed. The results showed that the MBSM can produce much finer powders compared to hammer milling, with particles demonstrating unique morphology and high specific surface area. Green wood milling yielded particles with the highest sphericity (0.64), aspect ratio (0.58), and micropore diameter (4.5 nm). Finer particles with spherical shapes enhanced the bulk density. Moreover, mill settings permit tailor-made powders according to the desired PSD.

1. Introduction

The transition from the fossil-based economy to a circular and sustainable bioeconomy relies on greater utilisation of renewable

biomaterials and the phasing out of fossil-based feedstock [1]. Wood powders are used in many different industrial applications such as refinement of bio-based platform chemicals [2,3], additive manufacturing (3D printing) [4], paperboard production [5], paper

^{*} Corresponding author.

E-mail address: atanu.kumar.das@slu.se (A.K. Das).

<https://doi.org/10.1016/j.powtec.2022.117664>

Received 31 March 2022; Received in revised form 15 June 2022; Accepted 19 June 2022

Available online 22 June 2022

0032-5910/© 2022 The Author(s). Published by Elsevier B.V. This is an open access article under the CC BY license (<http://creativecommons.org/licenses/by/4.0/>).

making [6], water treatment [7,8], fuel pellet production [9] and the manufacture of wood-based composites, wood plastic composites (WPC) and particleboard [10–12]. In these applications, their physical structure and chemical composition are often important considerations.

Wood powders consist of particles of different shapes and sizes; the application sets the requirements for the desired particle specifications. The size reduction method leaves its signature on particle morphology, including the surface distribution of wood's macromolecular components, an influential factor in applications [13]. A large specific surface area and high porosity enhance reaction chemistry by facilitating penetration of chemicals and enzymes [14]. As particle size decreases, so does cellulose crystallinity [15] and this increases specific surface area [14] and has benefits, for example, when converting cellulose to glucose via hydrolysis. Improved conversion of glucose has also been observed from finely milled oak [16] and loblolly pine [3] compared to coarser powders. Improved isolation of macromolecular components is correlated to the fineness of wood particulates [17] and are important for the extraction of lignin [18,19].

Particle size is also important for thermal conversion processes using wood as it affects heat transfer and the rate of devolatilisation. Effective (pulverised-fuel) boiler performance in co-firing wood, requires that particles should be <1 mm in diameter for optimal combustion efficiency [20]. During pyrolysis, particle size influences reaction and heating rates [21] and directly affects carbon yield in the char product [22]. Smaller particle diameters lead to enhanced bio-oil [23] and tar yields [21] due to a reduction in vapour-phase residence time and the suppression of char-forming reactions [24].

Wood powders can be produced from a range of mill types that usually operate with pre-dried feedstock. The resulting particle size distribution (PSD) of a powder depends on the comminution technology employed [25]. For example, the particle size can be controlled to some extent using different rotation speeds and actuators in hammer mills (e.g. the number of hammers [26]). The common two-stage hammer mill can generally produce a wood powder with PSD below 1 mm (sieving, mass basis) from pre-dried wood chips [20]. Knife mills can also reduce pre-dried chips to a powder with PSD below 1.5 mm [27].

Hammer mill powders have narrow elongated particles with angular profiles; this shape could be classified as a regular shape for wood powders. Knife mills, on the other hand, yield particles with rectangular shapes [28]. The bulk densities of powders are affected by their particle morphologies. Thin and long or hook-shaped particles increase the tendency of the powder to bridge [28]. This and large interparticle voids can lead to low packing efficiency. Although optimal packing is a complex problem, smaller particles diameters, tending towards spherical shapes, increase packing because of their ability to more freely move and fill gaps [29]. Therefore, in addition to the particle density and porosity, shape also plays a role in the bulk density of wood powders.

Due to the large data sets that come with studying PSDs of powders, statistical tools have been used to develop models on powder quality. MODDE Pro-12 software has been employed for investigating wood powder properties, i.e., PSD and bulk density using multi-linear regression (MLR) models [30]. The authors have used MLR models to investigate the effect of moisture content, feeding speed, and sawblade speed on energy requirements, PSD, and bulk density. Tukey's model with SAS 9.0 software has been used by Jiang et al. [31] to study the effect of moisture content in the feedstock material on powder PSD. Others have used Levenberg-Marquardt's non-linear regression model to investigate the correlation and model fitness for energy consumption, Hausner ratio, and Carr-compressibility index in relation to particle size [32]. Artificial neural network (ANN) models using back propagation (Levenberg-Marquardt) algorithms have been described to understand the relationship between energy consumption, powder moisture content, and powder size [29].

In this study, the impact of a new type of green milling technology on wood powder properties was investigated. The influence of shape properties on the bulk density of powders was studied. The effect of

wood moisture content, at the time of milling, on wood powder properties and the relationship between shape properties and bulk density of wood powder were analysed using a statistical tool. The shape, size, surface area, and porosity of powders were characterised. The effect of green versus dry milling of wood on particle properties and the bulk density of powders was also examined.

2. Materials and methods

Pine (*Pinus sylvestris* L.) wood powders used in this study were obtained from a series of designed experiments using a prototype multi-blade shaft mill (MBSM) [30]. There were nine types of powders corresponding to nine different mill settings. The ranges of experimental used parameters for wood moisture contents, feeding speeds and blade speeds were 10–50% (wet basis), 1.3–2.6 m min⁻¹ and 52–72 m s⁻¹, respectively. Hammer mill powders were produced from a single setting for the purpose of comparison.

2.1. Representative material sampling

The wood powder samples were sieved by a sieve shaker (Analysette 3, Fritsch, Germany) set at 1.5 mm amplitude for 10 min to obtain ≤1.0 mm particles prior to sampling by rotary sample divider for image, surface area and porosity analyses.

2.2. Two dimensional image analysis

Particle size distributions and shapes of powders were characterised with a 2D image analyser (CAMSIZER XT Particle Analyser, Microtrac RETSCH GMBH, Germany) with a designed size detection range of 0.001 to 3.0 mm at the Department of Engineering Sciences and Mathematics, Luleå University of Science and Technology, Luleå, Sweden. The image analyser used CAMSIZER XT 6.3.10 software (Microtrac RETSCH GMBH, Germany).

Three replicate samples were used for each powder type, resulting in 81 experiments with the image analyser, each producing a spectrum of data on power particle size distribution (PSD) and particle shape factors. In the analysis, the three replicates data sets were averaged. The sample sizes used in this study were 2.8–6.1 g. The software calculated the PSD and shape factors using the following relations [33].

The frequency distribution over $X_{c \min}$ was used to analyse the results of particle size defined by Eq. (2):

$$Q_3(X_{c \min}) = \frac{dQ_3(X_{c \min})}{X(X_{c \min})} \quad (1)$$

In which $X_{c \min}$ is the shortest chord among several chords of a particle (Fig. 1a), Q_3 is the cumulative size distribution based on volume.

$$P_3(X_{c \min}) = dQ_3(X_{c \min}) \quad (2)$$

Where, P_3 is particle size distribution based on volume.

The aspect ratio and sphericity were used to characterise the shape of particles. The aspect ratio is the ratio of particle width (X_b) to particle

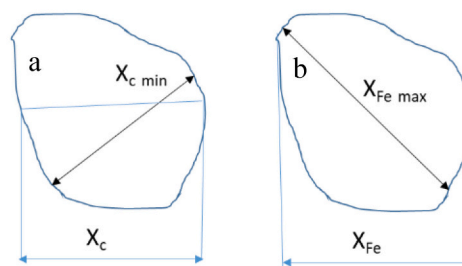


Fig. 1. Shape quantification parameters a) chord of the particle and b) Feret diameter.

length (X_l) defined by Eq. (3).

$$\text{Aspect ratio} = \frac{X_b}{X_l} \quad (3)$$

Where, X_b is the $X_{c \min}$ and X_l is the $X_{Fe \max}$. $X_{c \min}$ is used to represent the width or breadth of a particle [33] whereas $X_{Fe \max}$ is considered as the length of the particle [33,34]. Feret maximal diameter ($X_{Fe \max}$) is the longest Feret diameter (The distance of two tangents placed perpendicularly in the measuring direction) (Fig. 1b) [33].

The sphericity ψ (dimensionless) of a particle expresses the deviation in shape from a sphere and depends on the area of a particle projection (X_A) and the measured circumference (X_p). The closer the value is to one, the more spherical the particle. It was calculated by the following Eq. (4):

$$\psi = \frac{4\pi X_A}{X_p^2} \quad (4)$$

2.3. Geometric surface area

For a spherical particle, the simple geometric surface area A (m^2) and particle volume V (m^3) are calculated using (5) and (6) in which r (m) is the particle radius.

$$A = 4\pi r^2 \quad (5)$$

$$V = \frac{4}{3}\pi r^3 \quad (6)$$

The ratio of surface area to volume of a particle, with common terms eliminated, is (7)

$$\frac{A}{V} = \frac{4\pi r^2}{\frac{4}{3}\pi r^3} = \frac{3}{r} \quad (7)$$

As the radius of the particle approaches zero, the ratio approaches infinity. It follows that for a finite volume of material, the greater the reduction in particle size, the greater the generated surface area. The surface area of a powder A_p (m^2) consisting of n (particles) with a diameter d (m) is calculated with (8), in which A_d (m^2) is the surface area of a single particle with diameter d .

$$A_p = A_{d1}n_{d1} + A_{d2}n_{d2} + A_{d3}n_{d3}\dots = \sum_d A_d n_d \quad (8)$$

The number of particles of diameter d can be estimated from a particle size distribution determined through sieve analysis of a representative powder sample (9) where M_d (kg) is the mass fraction of sieved particles at diameter d (from a unit mass sample) and m_d (kg) is the mass of a single particle.

$$n_d = \frac{M_d}{m_d} \quad (9)$$

The particle mass m_d is found from the relationship between volume (6) and material density (10) ρ (kg m^{-3}) with the substitution $r = d/2$, resulting in (11).

$$m_d = \rho V \quad (10)$$

$$n_d = \frac{M_d}{\rho \pi d^3} \quad (11)$$

With elimination of common terms, the surface area of the powder (8) can then be rewritten as (12).

$$A_p = \sum_d A_d n_d = \sum_d \left[4\pi (d/2)^2 \right] \left[\frac{M_d}{\rho \pi d^3} \right] = \frac{6}{\rho} \sum_d \frac{M_d}{d} \quad (12)$$

The surface area generation \dot{A} ($\text{m}^2 \text{ kWh}^{-1}$) of size reduction can be calculated from the specific milling energy e_M (kWh t^{-1}) on a dry mass basis (13).

$$\dot{A} = e_M \cdot A_p^{-1} \quad (13)$$

2.4. Measured surface area and porosity

Specific surface area (i.e. BET) of powders and porosity were determined for three powder types; i) the MBSM powder from wet wood with lowest bulk density, ii) the MBSM powder from dry wood with highest bulk density and iii) the hammer mill powder. Sample sizes ranged from 1.1 to 1.3 g. Analysis was carried out by Celnis Analytical, Ireland, using a NOVA 2200e series surface area and pore size analyser (Quantachrome Instruments, Boynton Beach, USA).

2.5. Statistical analysis

Wood powder properties, i.e., aspect ratio and bulk density were evaluated by orthogonal partial least squares projections to latent structures (OPLS) [35] and orthogonal partial least squares discriminant analysis (OPLS-DA) [36] using SIMCA 16 software (Umetrics, Umeå, Sweden). Prior to model construction of shape factors, the PSD was limited to 50 to 500 μm because of having poor statistics beyond the range (suggestion from expert of Microtrac RETSCH GMBH). All data were subsequently mean centred and scaled to equal variance (denoted UV-scaling in SIMCA). In the following modeling, the image analysis data (aspect ratio) was put in a matrix (X), and the measured responses, i.e., powder bulk density, were arranged in a matrix (Y). Moreover, the observations were divided into two groups (denoted class 1 & 2) based on initial wood moisture content. An initial principal component analysis (PCA) was conducted on each specific dataset (X) to evaluate general trends and patterns in the data and outlier detection. Cross-validation (venetian blinds) was used for evaluating the calibration (OPLS) and discriminant models (OPLS-DA) by the following diagnostics; R^2 (coefficient of determination, describing the amount of explained variation in X), Q^2 (coefficient of multiple determination, describing the amount of variation in the cross-validated subsets predicted by the model) and RMSECV (root mean square error using cross-validation, using seven cross validation groups and same number of iterations).

3. Results and discussion

3.1. Particle size distribution

The particle size distribution of MBSM powders and hammer mill powder is presented in Fig. 2. The peaks of the MBSM distributions occur in the range of 30 to 300 μm . The magnitudes of the peaks for MBSM powders are much greater and substantially narrower than that of the hammer mill powder, indicating substantially finer powders. The cumulative volume percent (insert graph) of particles <0.5 mm in MBSM powders was therefore much higher; 68.4 to 87.5% for MBSM versus 48.2% for hammer mill. In other words, there were almost twice the amount of finer particles in MBSM powders. The >1.0 mm particles for MBSM powders were 5 to 18% only depending on the mill settings and wood moisture content.

The two narrowest PSDs (C and H) were observed from both low and high moisture content wood with high blade speed and low feeding speed. The broadest PSD was observed for the MBSM settings of low moisture content with low blade speed and high feeding speed (B). BS and FS affect the PSD (peak width) and gradual transition from I to E are results of their different settings.

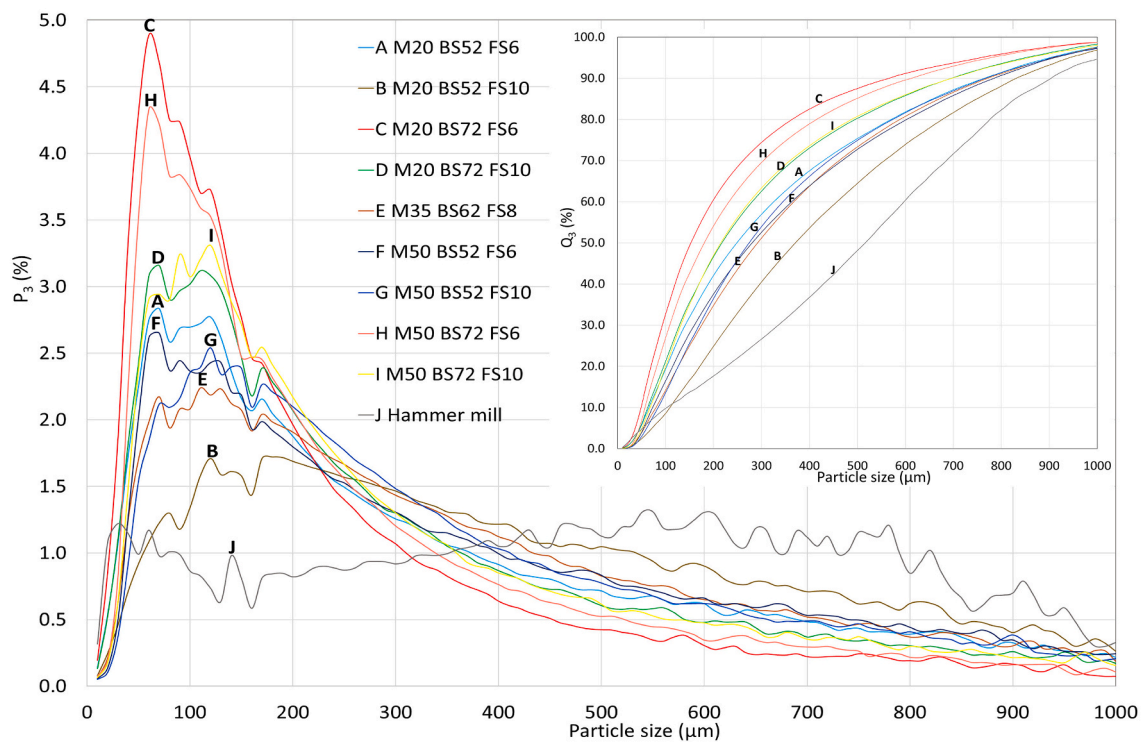


Fig. 2. Particle size distribution (P_3) of powders obtained from the multi-blade shaft mill and hammer mill. The inserted graph is the cumulative particle size distribution (Q_3). Symbols refer to M = moisture content (% wet basis), BS = blade speed (m s^{-1}) and FS = log feeding speed (m min^{-1}).

These results (volume basis) generally agree with those from mechanical sieving analysis (mass basis) of MBSM powders [30]. They show that the wood moisture content and the MBSM blade speed produce similar effects on produced powders and that these differences are small compared to the differences between MBSM and hammer mill powders.

3.2. Particle shape analysis

The aspect ratio and sphericity of powders are presenting in Fig. 3, in which MBSM data is coloured according to the moisture content of the wood used in milling (i.e. green and brown representing above and below fibre saturation point, respectively). MBSM powders obtained using different milling parameters did not show significant shape differences. The values of aspect ratio and sphericity of MBSM powders were higher than hammer-milled powders. The range of aspect ratio and sphericity were 0.54–0.61 (0.57) and 0.51 to 0.75 (0.63), respectively for MBSM powders across MBSM parameter settings. The mean aspect ratio and sphericity of hammer-milled powders were 0.41 and 0.54, respectively.

The moisture content during milling is the primary factor that determines particle shape factors of MBSM powders. This is evident by observing how high (green) and low (brown) moisture content data is differentiated from each other in two discrete bundles of curves (Fig. 3). For both shape factors, there is a clear crossover point in the data at approximately 200 μm (crossover region 150–250 μm). Above this point, high moisture content yields powders with greater aspect ratio and sphericity. Below the crossover, low moisture yielded greater aspect ratio and sphericity. The shape factors for the experimental mid-point (dotted line) in the experiments were approximately intermediate

between the bundles. Both shape factors of hammer-milled powders display similar behaviour and slope at different particle sizes.

The method of drying of wood powders may be a factor in this behaviour. Uneven moisture distribution in wood during drying causes internal stress due to moisture gradient leading to wood deformation [37]. This is analogous to the warping of pine boards due to internal stress while drying [38]. Trubetskaya et al. [39] observed that pine wood particles became both more spherical during rapid devolatilisation and more porous with more inner cavities. Despite the lower temperature used in drying herein, this explanation may aid the understanding of how particle shape is affected by moisture removal. Further studies are needed to investigate the morphological change of the smaller particles below the size of crossover region.

The obtained MBSM powders had higher aspect ratio and sphericity compared to those in previous studies. Aspect ratios and sphericity in hammer mill pine powders were found to be 0.21–0.22 and 0.44–0.45 for a particle size distribution of 3.2–25.4 mm [32]. Kobayashi et al. [40] found aspect ratio 0.20–0.33 for 0.02–0.5 mm pine powder milled in a vibration mill (rod and ball mill).

3.3. Surface area, porosity and powder bulk density

The measured results of surface area and porosity by BET analysis for the MBSM powders with the lowest (green wood) and highest (dry wood) bulk density and that of the hammer mill powder are presented in Table 1. The MBSM powder (green wood) showed 3.2 times higher specific surface area compared to hammer mill powders (1.378 vs. 0.4291) and 2.5 times higher surface area than MBSM powder (dry wood) (1.378 vs. 0.5573).

MBSM powders from green wood demonstrated 2.7 times (0.002759

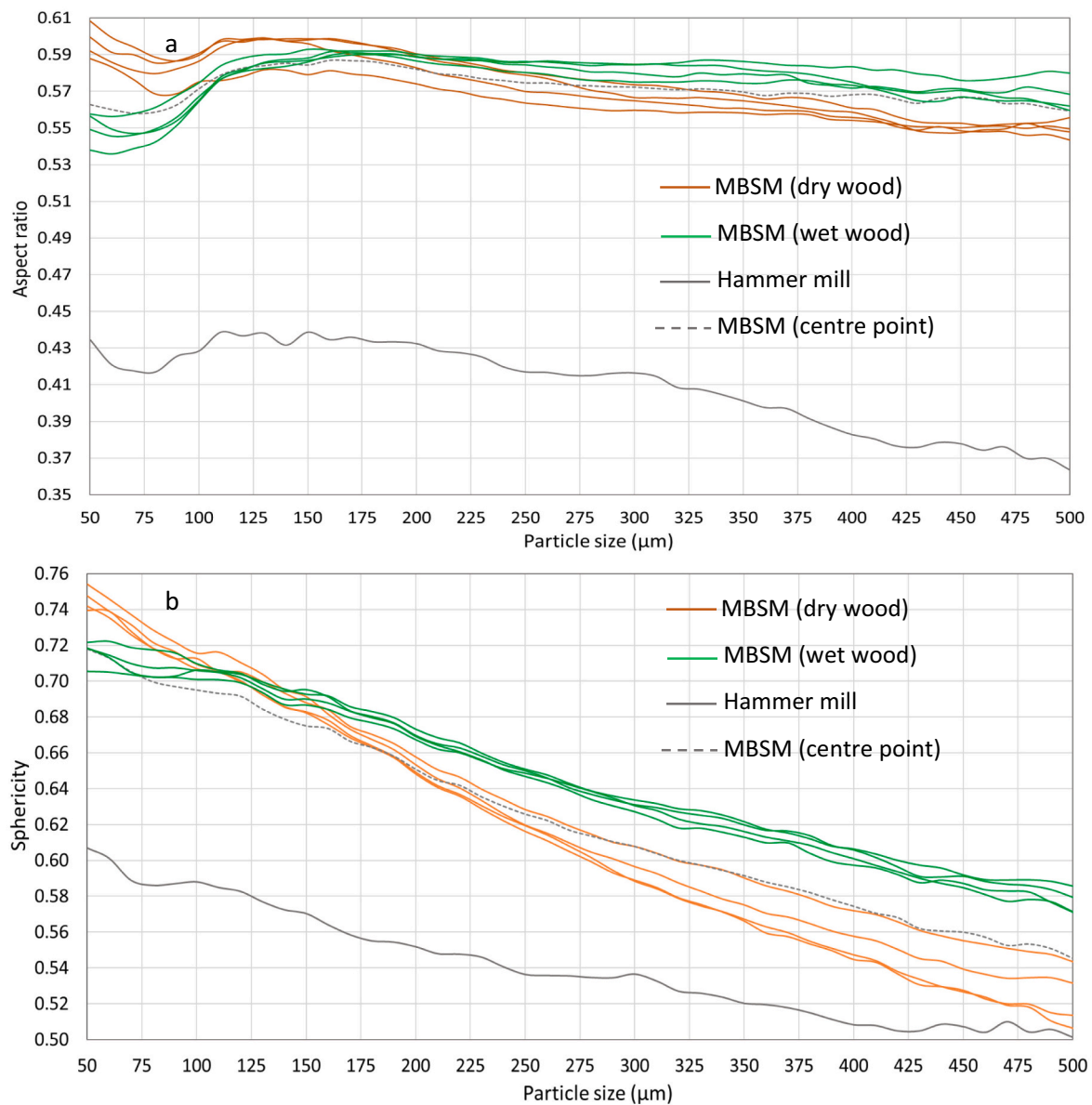


Fig. 3. Aspect ratio (a) and sphericity (b) of multi-blade shaft mill (MBSM) and hammer mill powder.

Table 1

Results from surface area and porosity analysis.

Sample description	Sample mass (g)	BET specific surface area (m ² g ⁻¹)	Pore volume (cm ³ g ⁻¹)	Average pore dia. (nm)	BJH method dia. (nm)	QSDFT micropore dia. (nm)	Specific milling energy, dry mass (kWh t ⁻¹) [30]	BET surface area generation (m ² kWh ⁻¹)	Geometric surface area generation (m ² kWh ⁻¹)
MBSM, N17L31 (green wood, lowest bulk density)	1.13	1.378	0.002759	8.012	3.542	4.52	197.4	6981	354
MBSM, N27L13 (dry wood, highest bulk density)	1.32	0.5573	0.001035	7.428	3.536	1.611	197.2	2826	374
Hammer mill	1.06	0.4291	0.001037	9.666	3.539	1.478	86.0	4990	588

vs 0.001037) greater pore volume and 3.1 times larger micropore diameter than hammer-milled powders (4.52 vs. 1.478). The porosity of MBSM green wood powders was 2.8 times higher than MBSM dry wood powders and 3.1 times higher than hammer mill powder. This indicates high porosity, which directly influences the bulk density of a material; the higher the porosity, the greater the volume occupied by the particles and the lower the bulk density of the material.

According to BET analysis, the milling of green wood in the MBSM yielded the greatest surface area per input of milling energy (Eq. 13), 40% more than hammer milling; the surface area generation was found to be 6981, 2826 and 4990 $\text{m}^2 \text{kWh}^{-1}$ for green wood, dry wood MBSM powders and hammer mill powders, respectively (Table 1). Based on the sieve results, this can be compared to the calculated geometric surface area generation which were found to be an order of magnitude lower (354, 374 and 588, respectively). This is only to be expected of smooth (pore-free) spheres, on which this simple calculation is based. However, it demonstrates the importance of porosity and particle morphology in the generation of surface area in powders.

Nopens et al. [41] have measured the specific surface area of Scots pine (*Pinus sylvestris*) wood. The authors used an original wood sample with a thickness of 1.5 mm. The obtained result showed a BET surface area of 1.533 $\text{m}^2 \text{g}^{-1}$. This value is similar to MBSM powders obtained from the green wood, although the instrument is different. It indicates that green milling can preserve the native structure of wood. This may contribute to a higher yield of value-added products, i.e., biochemical in the downstream process.

Earlier results showed that the bulk density of dry MBSM powders was only dependent on the wood moisture content at the time of milling (Table S). OPLS analysis of the bulk density mirrored this finding and showed that data form two distinct groups of green (above fibre saturation point) and dry wood (below fibre saturation point) (Fig. 4a,b). OPLS-DA analysis showed that the aspect ratio of powder obtained from dry wood was clearly separated from wet (Fig. 4a). The aspect ratio was higher for smaller particles from dry wood, while it was higher for bigger particles from green wood. This trend can also be observed in Fig. 3, where powder from dried wood had a higher aspect ratio for smaller particles. The produced models show that aspect ratio and bulk density ($R^2 = 0.87$, $Q^2 = 0.80$, and $\text{RMSEcv} = 17.31$) (Fig. 4b) and particle number and bulk density ($R^2 = 0.86$, $Q^2 = 0.84$, and $\text{RMSEcv} = 15.58$) are well correlated (Fig. S). The bulk density increased with the

increase of aspect ratio and powder sourced from dry wood showed higher aspect ratio and bulk density (Fig. 4b).

The large differences in bulk density are attributed to the differences in aspect ratio between powders. It could also be influenced by packing efficiency, being a function of differences in particle shapes, but the evidence for this is absent in this study. For example, others have found that smaller particles can move easily and have the ability to fill up the spaces between the bigger particles [29]. In this study, the number of smaller size particles were higher for powder obtained from dry wood. Although the aspect ratio was higher and lower for dry and green wood (Figs. 3 and 4a), the higher number of smaller particles with higher aspect ratio was comparatively more for powders obtained from dry wood (for the size range 20–150 μm , there were approximately 67,000 particles g^{-1} from the driest wood compared to 38,000 particles g^{-1} from green). Therefore, the finer particles with more spherical shape (and less porosity) in powders from dry wood enhance the homogenous distribution by filling the gaps between the bigger particles and increase the compactness of powder leading to a higher density.

Nevertheless, the inherent chemical composition, for example due to varying amounts of extractives present with moisture in the wood, due to using dry and green materials may have an impact on the findings in this study. Future microscopic studies combined with chemical analysis methods may shed more light on these possible factors.

4. Conclusions

This study showed that multi-blade milling enabled unique powder production from a single-step size reduction operation. Produced wood powders were much finer with unique particle morphology compared to a reference hammer mill powder. They exhibited a higher aspect ratio, sphericity, specific surface area, pore volume, and micropore diameter. Moreover, the higher aspect ratio and sphericity of MBSM powders were observed, for the majority of the studied particle size distribution, when milling green wood. Finer particles with spherical shapes had influential factors enhancing the packing effectiveness leading to the bulk densities values. Furthermore, the multi-blade mill operational parameters did not affect, to any great extent, the shape factors of powders – leading to the conclusion that the observed particle morphology is a characteristic of this size reduction technology. Future research is needed to fully characterise the microstructure of MBSM powders but the evidence

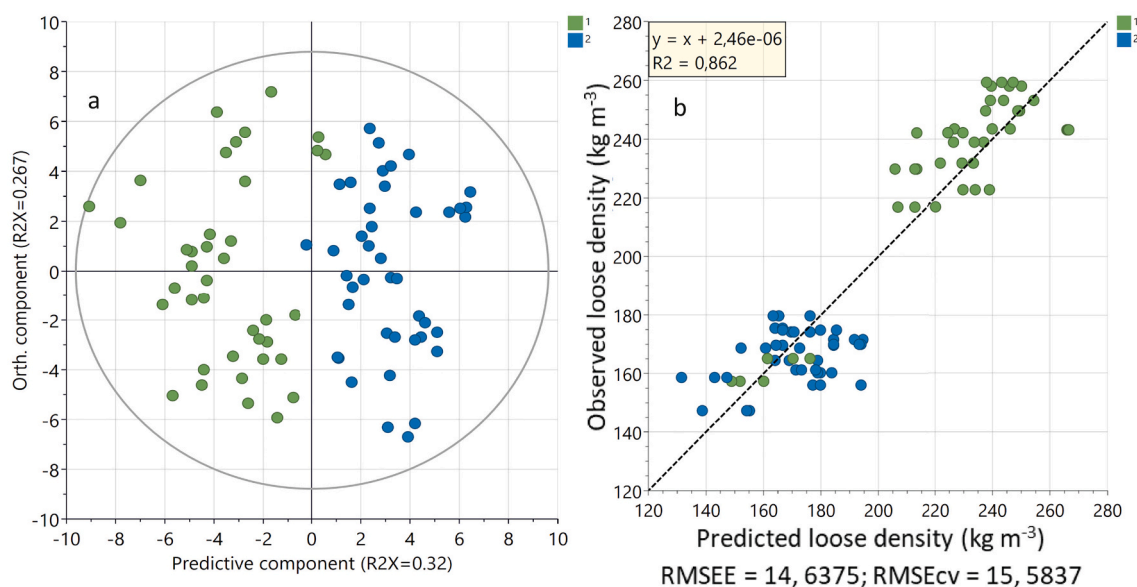


Fig. 4. (a) Score plot derived from class discriminant analysis (OPLS-DA) of AR dependence on moisture content (dry (class 1, green) and wet (class 2, blue), and (b) OPLS calibration model for aspect ratio (X) and bulk density (Y) displaying measured bulk density (kg m^{-3}) versus model predicted bulk density (kg m^{-3}). (For interpretation of the references to colour in this figure legend, the reader is referred to the web version of this article.)

suggests that their observed low bulk density from green milling can be attributed to significant differences in particle morphology and porosity.

Nomenclature

A	geometric surface area (m^2)
A_d	geometric surface area of single particle of diameter d (m^2)
A_p	geometric surface area of a powder (m^2)
\dot{A}	surface area generation of size reduction ($m^2 \text{ kWh}^{-1}$)
ANN	artificial neural network
BS	blade speed ($m \text{ s}^{-1}$)
d	particle diameter (m)
e_M	specific milling energy, dry mass (kWh t^{-1})
FS	log feeding speed ($m \text{ min}^{-1}$)
M	moisture content of wood (%)
MBSM	multi-blade shaft mill
MLR	multi-linear regression
M_d	mass fraction of sieved particles at diameter d (kg)
m_d	mass of a single particle (kg)
n_d	number of particles of diameter d (particles)
OPLS	calibration model
OPLS-DA	discriminant model
PSD	particle size distribution
P_3	volume based particle size distribution
Q^2	coefficient of multiple determination
Q_3	volume based cumulative distribution (% passing)
dQ_3	difference of two consecutive values of Q_3
R^2	coefficient of determination
r	particle radius (m)
RMSECV	root mean square error using cross-validation
V	particle volume (m^3)
X_A	area of a particle projection (mm^2)
X_b	particle width (mm)
$X_{c \text{ min}}$	width (mm)
$X_{Fe \text{ max}}$	particle length (mm) (Feret maximal diameter)
X_l	particle length (mm)
X_p	measured circumference
ψ	sphericity (dimensionless)
ρ	material density ($kg \text{ m}^{-3}$)
WPC	wood plastic composites

Funding

This study was funded in part by the Swedish Energy Agency (Project number- 46904-1) and the Swedish Bio4Energy Strategic Research Environment. Funding from the Department of Forest Biomaterials and Technology at the Swedish University of Agricultural Sciences is also acknowledged.

CRediT authorship contribution statement

Atanu Kumar Das: Conceptualization, Methodology, Software, Formal analysis, Investigation, Data curation, Writing – original draft, Writing – review & editing, Visualization. **David A. Agar:** Conceptualization, Methodology, Validation, Formal analysis, Writing – original draft, Writing – review & editing, Visualization, Supervision, Funding acquisition. **Mikael Thyrel:** Formal analysis, Writing – review & editing. **Magnus Rudolfsson:** Conceptualization, Methodology, Validation, Formal analysis, Writing – review & editing, Visualization, Supervision, Project administration, Funding acquisition.

Declaration of Competing Interest

The authors declare that they have no known competing financial interests or personal relationships that could have appeared to influence the work reported in this paper.

Acknowledgments

The authors thank Gunnar Kalén and Markus Segerström of the Biomass Technology Centre and Professor Kentaro Umeki of Luleå University of Technology. Sven Bremenfeld and Ted Rönnevall of Microtrac Retsch GmbH are warmly acknowledged for technical consultation.

Appendix A. Supplementary data

Supplementary data to this article can be found online at <https://doi.org/10.1016/j.powtec.2022.117664>.

References

- [1] U. Fritsche, G. Brunori, D. Chiaramonti, C. Galanakis, S. Hellweg, R. Matthews, C. Panoutsou, Future Transitions for the Bioeconomy towards Sustainable Development and a Climate-Neutral Economy, Luxembourg, 2020.
- [2] M. Zhang, X. Song, T.W. Deines, Z.J. Pei, D. Wang, Biofuel manufacturing from woody biomass: effects of sieve size used in biomass size reduction, *J. Biomed. Biotechnol.* 2012 (2012).
- [3] U.P. Agarwal, J.Y. Zhu, S.A. Ralph, Enzymatic hydrolysis of loblolly pine: effects of cellulose crystallinity and delignification, *Holzforschung* 67 (2013) 371–377.
- [4] A.K. Das, D.A. Agar, M. Rudolfsson, S.H. Larsson, A review on wood powders in 3D printing: processes, properties and potential applications, *J. Mater. Res. Technol.* 15 (2021) 241–255.
- [5] S.Y. Kim, J.Y. Lee, C.H. Kim, G.B. Lim, J.H. Park, E.H. Kim, Surface modifications of organic fillers to improve the strength of paperboard, *Bioresources* 10 (2015) 1174–1185.
- [6] C.H. Kim, J.Y. Lee, Y.R. Lee, H.K. Chung, K.K. Back, H.J. Lee, H.J. Gwak, H. R. Gang, S.H. Kim, Fundamental study on developing lignocellulosic fillers for papermaking(II) - effect of lignocellulosic fillers on paper properties, *Palpu Chongi Gisul/J. Korea Tech. Assoc. Pulp Paper Indus.* 41 (2009) 1–6.
- [7] H. Sillerova, M. Komarek, V. Chrastny, M. Novak, A. Vanek, O. Drabek, Brewers draf as a new low-cost sorbent for chromium (VI): comparison with other biosorbents, *J. Colloid Interface Sci.* 396 (2013) 227–233.
- [8] A. Keranen, T. Leiviska, B.Y. Gao, O. Hormi, J. Tanskanen, Preparation of novel anion exchangers from pine sawdust and bark, spruce bark, birch bark and peat for the removal of nitrate, *Chem. Eng. Sci.* 98 (2013) 59–68.
- [9] D.A. Agar, M. Rudolfsson, G. Kalen, M. Campargue, D.D. Perez, S.H. Larsson, A systematic study of ring-die pellet production from forest and agricultural biomass, *Fuel Process. Technol.* 180 (2018) 47–55.
- [10] E.D.B. Ferreira, C.B.B. Luna, E.M. Araujo, D.D. Siqueira, R.M.R. Wellen, Polypropylene/wood powder/ethylene propylene diene monomer rubber-maleic anhydride composites: effect of PP melt flow index on the thermal, mechanical, thermomechanical, water absorption, and morphological parameters, *Polym. Compos.* 42 (2021) 484–497.
- [11] K. Renner, C. Kenyo, J. Moczo, B. Pukanszky, Micromechanical deformation processes in PP/wood composites: particle characteristics, adhesion, mechanisms, *Compos. Part A-Appl. Sci. Manuf.* 41 (2010) 1653–1661.
- [12] S.H. Tian, Y.F. Luo, J.Z. Chen, H. He, Y. Chen, Z. Ling, A comprehensive study on the accelerated weathering properties of polypropylene-wood composites with non-metallic materials of waste-printed circuit board powders, *Materials* 12 (2019).
- [13] P. Karinkanta, A. Ammala, M. Illikainen, J. Niinimäki, Fine grinding of wood - overview from wood breakage to applications, *Biomass Bioenergy* 113 (2018) 31–44.
- [14] S.D. Mansfield, C. Mooney, J.N. Saddler, Substrate and enzyme characteristics that limit cellulose hydrolysis, *Biotechnol. Prog.* 15 (1999) 804–816.
- [15] L. Zhu, J.P. O'Dwyer, V.S. Chang, C.B. Grandia, M.T. Holtzapfel, Structural features affecting biomass enzymatic digestibility, *Bioresour. Technol.* 99 (2008) 3817–3828.
- [16] R.K. Dasari, R.E. Berson, The effect of particle size on hydrolysis reaction rates and rheological properties in cellulosic slurries, *Appl. Biochem. Biotechnol.* 137 (2007) 289–299.
- [17] K. Sarkanen, C.H. Ludwig, *Lignins: Occurrence, Formation, Structure and Reactions*, 1971.
- [18] M. Funaoka, S. Fukatsu, Characteristics of lignin structural conversion in a phase-separative reaction system composed of cresol and sulfuric acid, *Holzforschung* 50 (1996) 245–252.
- [19] M. Funaoka, M. Matsubara, N. Seki, S. Fukatsu, Conversion of native lignin to a highly phenolic functional polymer and its separation from lignocellulosics, *Biotechnol. Bioeng.* 46 (1995) 545–552.
- [20] L.S. Esteban, J.E. Carrasco, Evaluation of different strategies for pulverization of forest biomasses, *Powder Technol.* 166 (2006) 139–151.
- [21] H. Lu, E. Ip, J. Scott, P. Foster, M. Vickers, L.L. Baxter, Effects of particle shape and size on devolatilization of biomass particle, *Fuel* 89 (2010) 1156–1168.
- [22] L. Wang, M. Trninic, Ø. Skreiberg, M. Gronli, R. Considine, M.J. Antal, Is elevated pressure required to achieve a high fixed-carbon yield of charcoal from biomass? Part 1: round-Robin results for three different corncob materials, *Energy Fuel* 25 (2011) 3251–3265.

- [23] A.V. Bridgwater, Review of fast pyrolysis of biomass and product upgrading, *Biomass Bioenergy* 38 (2012) 68–94.
- [24] D. Agar, N. DeMartini, M. Hupa, Influence of elevated pressure on the torrefaction of wood, *Energy Fuel* 30 (2016) 2127–2136.
- [25] C. Mayer-Laigle, R.K. Rajaonarivony, N. Blanc, X. Rouau, Comminution of dry lignocellulosic biomass: part II. Technologies, improvement of milling performances, and security issues, *Bioengineering* 5 (2018) 50.
- [26] D.J. Schell, C. Harwood, Milling of lignocellulosic biomass - results of pilot-scale testing, *Appl. Biochem. Biotechnol.* 45-6 (1994) 159–168.
- [27] M. Phanphanich, S. Mani, Impact of torrefaction on the grindability and fuel characteristics of forest biomass, *Bioresour. Technol.* 102 (2011) 1246–1253.
- [28] S. Paulrud, J.E. Mattsson, C. Nilsson, Particle and handling characteristics of wood fuel powder: effects of different mills, *Fuel Process. Technol.* 76 (2002) 23–39.
- [29] M. Gil, I. Arauzo, E. Teruel, Influence of input biomass conditions and operational parameters on comminution of short-rotation forestry poplar and corn stover using neural networks, *Energy Fuel* 27 (2013) 2649–2659.
- [30] A.K. Das, D.A. Agar, S.H. Larsson, T. Holdo, D. Fernando, M. Rudolfsson, Multi-blade milling from log to powder in one step - experimental design and results, *Powder Technol.* 378 (2021) 593–601.
- [31] J.X. Jiang, J.W. Wang, X. Zhang, M. Wolcott, Microstructure change in wood cell wall fracture from mechanical pretreatment and its influence on enzymatic hydrolysis, *Ind. Crop. Prod.* 97 (2017) 498–508.
- [32] H. Rezaei, C.J. Lim, A. Lau, S. Sokhansanj, Size, shape and flow characterization of ground wood chip and ground wood pellet particles, *Powder Technol.* 301 (2016) 737–746.
- [33] R. Technology, CAMSIZER[®] Characteristics, DIN 66141Rheinische Strasse 43 42781 Haan Germany, 2009.
- [34] H.G. Merkus, *Fundamentals, Practice, Quality, Particle Size Measurements*, Springer, Netherlands, 2009 (pp. XII, 534).
- [35] J. Trygg, S. Wold, Orthogonal projections to latent structures (O-PLS), *J. Chemom.* 16 (2002) 119–128.
- [36] M. Bylesjo, M. Rantalainen, O. Cloarec, J.K. Nicholson, E. Holmes, J. Trygg, OPLS discriminant analysis: combining the strengths of PLS-DA and SIMCA classification, *J. Chemom.* 20 (2006) 341–351.
- [37] H.J. Chai, C. Xu, J. Li, F.X. Kong, Y.C. Cai, Effects of pretreatment with saturated wet air and steaming on the high-frequency vacuum drying characteristics of wood, *Bioresources* 14 (2019) 9601–9610.
- [38] J. Couceiro, L. Hansson, M. Sehlstedt-Persson, T. Vikberg, D. Sandberg, The conditioning regime in industrial drying of scots pine sawn timber studied by X-ray computed tomography: a case-study, *Eur. J. Wood Wood Prod.* 78 (2020) 673–682.
- [39] A. Trubetskaya, P.A. Jensen, A.D. Jensen, A.D.G. Llamas, K. Umeki, P. Glarborg, Effect of fast pyrolysis conditions on biomass solid residues at high temperatures, *Fuel Process. Technol.* 143 (2016) 118–129.
- [40] N. Kobayashi, T. Sato, N. Okada, J. Kobayashi, S. Hatano, Y. Itaya, S. Mori, Evaluation of wood powder property pulverized by a vibration mill, *Nihon Enerugi Gakkaishi/J. Jpn. Inst. Energy* 86 (2007) 730–735.
- [41] M. Nopens, U. Sazama, S. Konig, S. Kaschuro, A. Krause, M. Froba, Determination of mesopores in the wood cell wall at dry and wet state, *Sci. Rep.* 10 (2020).